Title: Sucrose transport and Sucrose Synthase activity control the source-sink relationship for biomass and grain yield in rice

Running Title: Source-sink relationship in cultivated and wild rice

Jyotirmaya Mathan, Anuradha Singh, Aashish Ranjan*

National Institute of Plant Genome Research, Aruna Asaf Ali Marg, New Delhi-110067, India.

***Corresponding Author**

e-mail: aranjan@nipgr.ac.in

Phone no. +91-11-26735117

Authors' email

Jyotirmaya Mathan: jyotirmaya@nipgr.ac.in

Anuradha Singh: annusingh1206@gmail.com

Date of submission: 19th October 2020

Number of figures: 7 figures

The word count: 5,085

Supplementary data: 10 supplementary figures and 1 supplementary table

Title: Sucrose transport and Sucrose Synthase activity control the source-sink relationship for biomass and grain yield in rice

Running Title: Source-sink relationship in cultivated and wild rice

Highlight

Differences in vascular features, sucrose transport, and Sucrose Synthase activity contribute to the differential source-sink relationship between the selected cultivated and wild rice that differ in biomass and grain yield.

Abstract

The source-sink relationship is key to overall crop performance. Detailed understanding of the factors that determine source-sink dynamics is imperative for the balance of biomass and grain yield in a crop plant. We investigated the differences in the source-sink relationship between a cultivated rice *Oryza sativa* cv. Nipponbare and a wild rice *Oryza australiensis* that show striking differences in biomass and grain yield. The wild rice, accumulating higher biomass, was not only photosynthetically efficient but also had efficient sucrose export from leaves. However, sucrose mobilization to the grains was limited due to impaired vasculature and sucrose transporter functions at the reproductive tissues of the wild rice. High cleavage activity of Sucrose Synthase followed by higher expression of Cellulose Synthase genes in the wild rice stem efficiently utilized photosynthates for the synthesis of structural carbohydrates, resulting in high biomass. In contrast, the source-sink relationship favored high grain yield in Nipponbare via accumulation of transitory starch in the stem, due to higher expression of starch biosynthetic genes, which is mobilized to panicles at the grain filling stage. Thus, sucrose transport along with functions of key sugar metabolic enzymes explained the differences in the source-sink relationship between the selected cultivated and wild rice.

Keywords: Biomass; Grain yield; Photosynthesis; Source-sink relationship; Starch; Structural carbohydrates; Sucrose synthase; Sucrose transport; Vascular features

68 **Introduction**

69 Source-sink relationship is critical for determining overall growth and performance of
70 crop plants (White *et al*., 2016). Photosynthetic carbon assimilation in source leaves, sucrose
71 transport through vasculature, type and strength of sink tissues, as well as metabolic status of
72 the tissues are the key features that determine the source-sink dynamics of a plant.
73 Photosynthetic leaves are the major source tissues of a plant, whereas types and efficiency of
74 sink organs vary depending upon the growth stages and environmental conditions. For
75 example, grains are the primary sink in the reproductive stage of crop plants, while roots,
76 stem/internodes, and growing leaves function as the sink in the vegetative stage. Natural
77 genetic variation for differences in the source-sink dynamics, resulting in changes in biomass
78 and yield, has been evident (Burnett *et al.*, 2016; White *et al.*, 2016; Fabre *et al.,* 2020). For
79 example, many of the wild relatives of rice accumulate high biomass with poor grain filling,
80 whereas cultivated varieties produce higher grain yield (Sanchez *et al.*, 2013).

81 Leaf morphological and anatomical features along with photosynthesis per unit leaf
82 area largely determine the source strength of a plant (Mathan *et al.*, 2016). Functions of the
83 key carbohydrate metabolic enzymes, such as ADP-glucose pyrophosphorylase (AGPase),
84 sucrose phosphate synthase (SPS), sucrose phosphate phosphatase (SPP) and Sucrose
85 synthase (SUS), are known to be key determinants of the metabolic status of source leaves
86 (Osorio *et al.*, 2014; Ruan, 2014). Similarly, the capacity to utilize photosynthates efficiently
87 largely determines the sink strength. Sink size, influenced by tiller number, spikelet number
88 per panicle, and seed size; and sink activity, determined by functions of various metabolic
89 enzymes such as cell wall invertase (cwINV) and sucrose synthase (SUS), dictate the
90 photosynthates utilization at a sink organ (Smith *et al.*, 2018; Stein and Granot, 2019).
91 Photosynthates are primarily partitioned from source leaves to different sink tissues in the
92 form of sucrose via phloem with the aid of SWEET and SUT transporters (Chen *et al.*, 2012;
93 Braun, 2012; Julius *et al.*, 2017). Mutations or overexpression of genes encoding sucrose
94 transporters affect plant yield and biomass via modulation of source-sink dynamics (Scofield
95 *et al.*, 2002; Chen *et al.*, 2012; Yang *et al.*, 2018). Besides the sucrose transporter functions,
96 vascular features not only determine the rate of sucrose export from leaf tissues to phloem
97 sap but also control mobilization of photosynthates to the panicles at the reproductive stage
98 (Qi *et al.*, 2008; Fujita *et al.*, 2013; Sack and Scoffoni, 2013).

99 Photosynthates assimilated in leaves are either used to meet immediate cellular needs
100 or mobilized into different sinks. Starch stored in leaves during the day, over and above the
101 immediate utilization and transport of photosynthates, is degraded during the night to be

102 transported to different sink organs for growth (Smith and Stitt, 2007; Chen *et al.*, 2012).
103 Mutants defective in sucrose transport, usually, accumulate starch in leaves at the end of the
104 night, limiting plant growth (Chen *et al.*, 2012). The utilization and storage of sugars are
105 regulated diurnally as well as developmentally. Stem serves as the main storage organ for
106 carbohydrates in crop plants, including rice, during vegetative growth. Sucrose, after getting
107 unloaded into the stem, could possibly be converted to different non-structural carbohydrates
108 (NSCs), such as glucose, fructose, and starch. Starch is reported to be the major storage form
109 in rice stem during the vegetative stage, which is mobilized to developing grains with the
110 onset of the reproductive stage, contributing up to half of the final grain yield (Wang *et al.*,
111 2017). A portion of the photosynthates is also used as a structural component of the cell wall
112 for the growth and development of new organs as well as elongation and thickening of
113 existing organs. High biomass accumulation is usually associated with accumulation of
114 cellulose and other structural carbohydrates in crop plants, with cellulose alone contributing
115 around 25-50% of plant biomass (Haigler *et al.*, 2001). Thus, the balance of structural and
116 non-structural carbohydrates derived from the sucrose in the stem is critical for determining
117 biomass and grain yield in cereal crops.

118 Sucrose, after reaching to the stem, is hydrolysed by two classes of enzymes,
119 Invertases (INV) and Sucrose Synthase (SUS). Invertases cleave sucrose into glucose and
120 fructose, while Sucrose Synthase (SUS) reversibly catalyses the formation of UDP-glucose
121 and fructose. The UDP-glucose, generated by the cleavage activity of SUS, is used as a
122 precursor for cellulose synthesis. Further, UDP-glucose can be converted to ADP-glucose for
123 usage in starch synthesis, making SUS a key enzyme for biomass and grain yield (Smith *et*
124 *al.*, 2012; Ruan, 2014; Stein and Granot, 2019). The functions of SUS is important for
125 phloem loading and unloading as well as for determining sink strength (Smith *et al.*, 2012;
126 Fan *et al.*, 2017; Yao *et al.*, 2020). Among the seven genes encoding SUS enzymes in rice,
127 *OsSUS1* and *OsSUS3* contribute to seed starch biosynthesis (Cho *et al.*, 2011). Higher
128 expression of *OsSUS3* also led to increased levels of structural carbohydrates, cellulose and
129 hemicellulose, in rice (Fan *et al.*, 2017). *OsSUS1* is highly expressed in rice internodes, with
130 a strong correlation with the expression pattern of genes encoding Cellulose Synthase,
131 *OsCES4*, *OsCES7*, and *OsCES9* (Hirose *et al.*, 2008; Guevara *et al.*, 2014). Among Cellulose
132 Synthase enzymes, OsCES4, OsCES7, and OsCES9 have been reported to function in
133 secondary cell wall formation (Tanaka *et al.*, 2003; Wang *et al.*, 2016). Thus, functions of
134 enzymes, such as INV, SUS and CES, are important for determining source-sink dynamics
135 for biomass and grain yield.

136 Despite the key importance of sucrose partitioning and metabolism in determining
137 source-sink relationship, this aspect is largely unexplored for optimization of grain yield and
138 biomass in rice. Cultivated rice varieties and their wild relatives, with striking differences in
139 yield and biomass traits, provide an excellent system to investigate the mechanistic basis of
140 the source-sink relationship. We investigated the limitations related to sucrose transport and
141 metabolism for grain yield in wild rice *O. australiensis*, resulting in higher biomass,
142 compared to the cultivated variety *O. sativa* cv. Nipponbare. We report higher accumulation
143 of structural carbohydrates, such as cellulose and hemicellulose, in the wild rice is due to
144 higher SUS cleavage activity together with higher expression of genes encoding Cellulose
145 Synthases. Cultivated rice, in contrast, accumulated more starch in the stem due to higher
146 expression of genes encoding starch biosynthesis enzymes. We also established the
147 contribution of specific sucrose transporters and vascular features towards impaired
148 mobilization of photosynthates to *O. australiensis* panicles.
149
150
151 **Materials and methods**
152 **Phenotyping of the selected rice accessions for biomass and yield-related traits**
153 Two cultivated varieties, *Oryza sativa* ssp. *indica* cv IR 64 and *Oryza sativa* ssp. *japonica* cv
154 Nipponbare, and three wild rice species, *Oryza rufipogon* (IRGC 99562), *Oryza latifolia*
155 (IRGC 99596), and *Oryza australiensis* (IRGC 105272), were grown in the experimental
156 field of National Institute of Plant Genome Research, New Delhi (*latitude* 28°36
157 N; *longitude* 77°12 E; *altitude* 216 m) under natural growing conditions. At least ten
158 individual plants of each genotype were used for phenotyping. Plant architectural traits were
159 quantified at the milk-stage of grain-filling. Seed traits, and fresh and dry weight were
160 quantified at grain maturity stage. Plant height was measured as the height from the soil
161 surface to the tip of central panicle; total leaves per plant, tiller number per plant, and
162 internode number per the main stem were counted manually; flag leaf width was quantified as
163 the width of the widest portion of the flag leaf; and internode length was calculated using the
164 distance between two consecutive nodes on the main stem. Stem width and circumference
165 were quantified using Fiji-Image J software from images of hand-cut sections of the same
166 region of the main stem. Fresh weight was quantified by directly weighing the entire plant
167 mass, and dry weight was quantified by weighing the dried plant mass after drying the entire
168 plant mass at 60°C for five days. Spikelet per panicle was counted manually, whereas seed
169 length and seed width (50 seeds per replicate) were measured using a digital Vernier calliper.

170 For seed weight analysis, 500-seeds were randomly selected and weighed using an electronic
171 balance. Raw data of biomass and grain yield-related traits for each genotype were
172 normalized to median from the entire sample set for principal Component analysis. Then, all
173 the data was converted on a log base 2 scale on JMP software from SAS
174 (https://www.jmp.com/en_us/home.html).
175
176 **Quantification of leaf photosynthesis rate and related physiological traits**
177 Leaf photosynthesis rate (A), stomatal conductance to water (g_sH_2O), and intercellular CO_2
178 concentration (C_i) were recorded from flag leaves at booting, and milk- and dough- stage of
179 grain filling for *O. sativa* ssp. *indica* cv. Nipponbare and *O. australiensis* using a portable
180 photosynthesis system LI-6400XT (LI-COR Biosciences). Data were recorded from at least
181 15 independent plants of each genotype on a clear day between 9.00 h to 11.00 h under
182 ambient CO_2 level (C_a; 400 µmol mol^{-1}), air temperature (30 ºC), leaf temperature (27 ºC),
183 and photosynthetic photon flux density (PPFD, 1,500 µmol m^{-2} s^{-1}) conditions.
184
185 **Quantification of glucose, fructose, and sucrose**
186 The non-structural carbohydrates (NSCs: glucose, fructose, and sucrose) present in the flag
187 leaf and stem were quantified for *O. sativa* ssp. *indica* cv. Nipponbare and *O. australiensis* at
188 the milk-stage of grain-filling by Gas Chromatography-Mass Spectrometry (GC/MS). Flag
189 leaf and stem tissues were harvested from field-grown plants of both the genotypes at 9:00-
190 11:00 am. For the quantification of NSCs in flag leaves at the end of the day (EOD) and end
191 of the night, tissue samples were collected at 6.00 pm and 6.00 am, respectively. The tissues
192 were sampled from at least four individual plants per genotypes and immediately frozen into
193 liquid nitrogen after harvesting. A 100 mg fresh weight (FW) of the tissues were extracted
194 using 1.0 ml water: chloroform: methanol (1:1:2.5) spiked with 10 µl internal standard (1 mg
195 ml^{-1} ribitol in water). The mixture was vortexed, centrifuged and 200 µl of polar phase were
196 dried for 3 hours in a speed-vac concentrator. Next, dried samples were derivatized with 50
197 µl of 20 mg ml^{-1} methoxyamine in pyridine warmed for 37°C for 120 mins with shaking.
198 Metabolites were further derivatized by adding 70 µl of N-methyl N-trimethylsilyl-
199 trifluoroacetamide (MSTFA) at 37°C for 30 min. Once derivatization was completed,
200 samples were transferred to GC compatible vials and 1µl of samples were injected on GC-
201 MS-QP2010 (Shimadzu) as described in Lisec *et al.* (2006). For metabolite identification, the
202 mass spectra were matched with commercially available spectral libraries NIST08, NIST11
203 and Wiley08 for automated peak identification and validated by retention index (RI) libraries

204 (http://gmd.mpimp-golm.mpg.de/). The relative amount of metabolites was presented by total
205 ion current signal which was normalized to Ribitol and tissue weight.
206
207 **Starch quantification**
208 Starch was quantified from flag leaves, stems, matured seeds, and different internodes of *O.*
209 *sativa* ssp. *indica* cv. Nipponbare and *O. australiensis*. The quantification of starch from flag
210 leaves and stems of the two genotypes were performed at the milk-stage of grain-filling at the
211 time of phenotyping of photosynthesis. In addition, flag leaves samples were used for starch
212 quantification at EOD and EON. Starch was also quantified from leaves at vegetative and
213 booting stage, as well as in different internodes of the two species at the milk-stage of grain-
214 filling. Starch was quantified using Mega-Calc Total starch determination kit (K-TSTA;
215 Megazyme) according to the manufacturer's protocol. Four independent biological replicates
216 were analysed for each tissue type for each genotype.
217
218 **^{14}C labelled sucrose loading assay**
219 The phloem loading capacity of ^{14}C labelled sucrose was quantified by following the method
220 as descried by Yadav *et al.* (2017). Briefly, rice flag leaves at milk-stage of grain-filling were
221 cut, and the leaf bases were immediately transferred to petri-dish submerged with MES/$CaCl_2$
222 buffer (20 mM MES, 2mM $CaCl_2$, pH 5.5 with KOH). Next, leaf discs (3.6 × 1.0 cm) were
223 excised using a cork borer, and immediately placed abaxial side down in the 24-well
224 microtiter plate pre-filled with 1 ml MES/$CaCl_2$ buffer spiked with 1mM sucrose solution
225 (1mM unlabelled Sucrose supplemented with 0.81µCi ml^{-1} ^{14}C Sucrose). Leaf discs
226 immersed in the above solution were vacuum-infiltrated for at least 20 min with gentle
227 shaking at room temperature. Labelled leaf discs were transferred to a fresh microtiter plate
228 and washed twice with 1.0 ml MES/$CaCl_2$ buffer, blot dried on absorbent filter paper, and
229 immediately frozen on dry ice and lyophilized. Next, ^{14}C sucrose loading capacity into leaves
230 was quantified by scintillation counting (PerkinElmer). Four leaf discs were used for each
231 biological replicate, and six biological replicates were used for each genotype per experiment.
232
233 **Sucrose quantification in phloem sap**
234 The amount of sucrose in the phloem was quantified using the EDTA-facilitated exudation
235 technique described by King and Zeevaart (1974). Flag leaves of the cultivated and wild rice
236 were excised at the milk-stage of grain-filling at around 9-10 am (when leaf photosynthesis
237 was quantified), leaf bases were immediately recut under exudation buffer (10 mM, Hepes,

238 10 mM EDTA, pH 7.5) to allow dispersion of any leaf contaminants, and placed in a 15 ml
239 tube containing 5 ml of the exudation buffer. Samples were incubated in a humid chamber
240 (relative humidity >90%) in the dark to prevent evapotranspiration, and exudates were
241 collected after 5 h of incubation. 2 ml of sample aliquots were spiked with 50 µl internal
242 standard (1 mg ml^{-1} ribitol in water), and freeze-dried for sucrose quantification using GC-
243 MS based method as described earlier. Individual flag leaves from different plants were
244 considered as separate biological replicates, and four biological replicates were analyzed for
245 each genotype.
246
247 **RNA isolation, cDNA synthesis and qRT-PCR analysis**
248 Total RNA from flag leaf, stem, and panicle base at milk-stage of grain-filling was extracted
249 using TRIzol reagent (Invitrogen), whereas RNA from spikelet at milk-stage was extracted
250 using plant RNA purification kit (Sigma-Aldrich) according to manufacturer's protocol. One
251 microgram (1µg) of total RNA was reverse transcribed to first strand-cDNA by anchored
252 oligodT priming using Thermo Scientific RevertAid cDNA synthesis kit following
253 manufacturer's instructions. The primer pairs (Table S1) of selected targeted genes used in
254 this study produced a single product as viewed through dissociation curve analysis. Further,
255 the efficiency of each primers was also evaluated using a standard curve method where five
256 cDNA quantities (1, 25, 50, 75, and 100 ng) from each genotype was used to construct a
257 standard curve, and efficiency were calculated using the formula $E = (10^{[-1/slope]}-1)*100$.
258 Expression analysis of each gene was performed at least in three biological replicates for each
259 genotype. The transcript levels of genes were normalized independently to two stable internal
260 controls actin (LOC_Os03g50885) and ubiquitin (LOC_Os03g03920) with similar results.
261 Relative expressions of target genes are presented using actin as the internal control applying
262 $2^{-\Delta Ct}$ method by Livak and Schmittgen (2001). *In sillico* expression analysis of the genes was
263 performed using OS_AFFY_RICE_6 dataset present in Genevestigator database
264 (https://genevestigator.com/gv/).
265
266 **Visualization and quantification of anatomical traits**
267 The vascular features of flag leaves as well as vascular bundles in the inner and outer ring of
268 the stem, and panicle base (0.5 cm above the panicle node) were visualized and quantified
269 through hand-cut transverse sections. Flag leaves, stems and panicle bases were hand-
270 sectioned using a razor-blade at the milk-stage of grain-filling, at least from five independent
271 plants for each genotype, and stained with toluidine blue O (0.02% toluidine blue O in water)

272 as described by Mitra and Loqué, (2014). Photographs were taken under a bright field
273 microscope (LMI). Quantification of the different anatomical traits were made using Fiji-
274 Image J software (Wayne Rasband, National Institute of Health).
275
276 **Cellulose staining and quantification**
277 For histochemical visualisation of cellulose, transverse hand-sections of rice stem
278 (approximately 20 µm thickness) at the milk-stage of grain-filling were stained using
279 calcofluor white (0.2% calcofluor white M2R in water) staining solution as described by
280 Ambavaram *et al.* (2011). Stained sections were photographed under UV light range using a
281 fluorescence microscope (excitation filter: 340-380 nm; Carl Zeiss Microscope). The
282 quantification of cellulose and hemicellulose was made using National Renewable Energy
283 Laboratory (NREL) protocols as described in Mund *et al.* (2016). The quantifications were
284 made in four biological replications for each genotype.
285
286 **Estimation of Sucrose synthase synthesis and cleavage activity**
287 The sucrose synthase (SUS) synthesis and cleavage activity were performed in stem tissue of
288 the two genotypes at the milk-stage of grain-filling. Tissue samples were homogenized in
289 extraction buffer (50 mM HEPES/NaOH (pH 7.5), 7.5 mM $MgCl_2$, 2 mM EDTA, 2% (w/v)
290 PEG 8000, 2% (w/v) PVP and 5 mM DDT) at 4 °C. The homogenate was centrifuged for 1
291 min at ~16,000 × *g*, the pellet was discarded and the crude extract was used for enzyme
292 assay. To quantify OsSUS synthesis activity, 50 µl of crude extract was incubated with 20
293 mM HEPES/NaOH buffer (pH 7.5), 5 mM $MgCl_2$, 20 mM KCl, 12 mM fructose, 0.4 mM
294 phosphoenolpyruvate, 2 mM uridine diphosphate UDP-glucose, 20 U pyruvate kinase, 20 U
295 lactate dehydrogenase, and 0.15 mM NADH in total 1.0 ml final reaction volume. Similarly,
296 to quantify OsSUS cleavage activity, 50 µl of crude extract was incubated with 20 mM
297 HEPES/NaOH buffer (pH 7.5), 100 mM sucrose, 2 mM UDP, 2mM $MgCl_2$, 0.005 UDP-
298 glucose dehydrogenase, and 1.5 mM NAD^+ in total 1.0 ml final reaction volume. The
299 reaction mixture was mixed gently, and decrease and increase in absorbance were recorded
300 for synthesis and cleavage activity, respectively, at 340 nm continuously for 0 to 300 sec
301 using a UV–Vis spectrophotometer. The OsSUS activity was calculated in terms of µmol
302 NADH oxidized (synthesis activity) and NAD+ reduced (cleavage activity) per min per mg
303 protein as described in Qazi *et al.* (2012).
304
305

306 **Subcellular localization of *OsSUS1***

307 Full length of *OsSUS1* CDS without stop codon was cloned under constitutive 35S promoter
308 with a C-terminal eYFP fusion into binary vector pEG10 (Earley *et al.*, 2006). The
309 recombinant plasmid along with empty vector control were then, introduced into EHA105
310 strain of *Agrobacterium tumefaciens*. Each transformant was co-infiltrated with a plasma
311 membrane-localized marker (PM-mCherry; Nelson *et al.*, 2007) into the leaves of *Nicotiana*
312 *benthamiana*. Confocal laser scanning microscopy TCS SP5 (Leica Microsystems) was used
313 to take the images with appropriate lasers.

314

315 **Results**

316 **Biomass and grain yield differences among the selected wild and cultivated rice**
317 **accessions**

318 We initiated the study with two cultivated rice varieties, *Oryza sativa* ssp. *japonica*
319 cv. Nipponbare and *Oryza sativa* ssp. *indica* cv. IR 64, and three wild relatives of rice, *Oryza*
320 *rufipogon*, *Oryza latifolia,* and *Oryza australiensis* that show remarkable variations in overall
321 growth and architectural features at both vegetative and reproductive stages (Fig. 1A). All the
322 selected wild rice species grew taller compared to the two cultivated varieties (Fig 1B).
323 Among all the accessions, *O. sativa* cv. Nipponbare produced lowest number of total leaves,
324 while *O. rufipogon* showed the highest number of leaves per plant (Fig. 1C). Nipponbare
325 showed a significantly lower number of leaves compared to all the selected wild species. In
326 addition, Nipponbare also showed significantly lower tiller number per plant compared to all
327 the selected accessions (Supplementary Fig. S1B). Selected wild rice species showed wider
328 leaves compared to the cultivated varieties, with *O. latifolia* showing widest leaves (Fig. 1D).
329 We, then, quantified number and length of internodes in the main stem, as internodes are
330 important contributors to the biomass of a plant. Cultivated rice varieties had fewer, smaller,
331 and slender internodes in the main stem compared to the wild accessions (Fig. 1E; and
332 Supplementary Fig. S1A, C). In addition, stem width and circumference were also lower for
333 Nipponbare and IR 64 compared to all selected wild species (Supplementary Fig. S1C, D).
334 Thus, plant architectural traits, such as height, branching, and internode features, as well as
335 leaf traits attributed to high biomass of the selected wild rice. Consistent with this, the
336 selected wild rice also showed higher fresh and dry weight compared to the cultivated
337 varieties. (Fig. 1F, G).

338 We, then, quantified seed traits of the selected cultivated and wild rice. The cultivated
339 rice varieties produced higher numbers of spikelets per panicle as well as higher seed weight

340 compared to the wild relatives (Fig. 1H, I). Higher seed weight of cultivated rice varieties
341 resulted due to longer and wider grains compared to the wild species (Supplementary Fig.
342 S1E, F). Principal Component analysis for all the quantified biomass and seed traits showed a
343 clear separation of wild and cultivated genotypes (Supplementary Fig. S2). Taken together,
344 these results confirmed the higher biomass accumulation at the expanse of grain yield in the
345 selected wild rice compared to the cultivated varieties. Wild rice *O. australiensis* had higher
346 phenotypic value for all the traits contributing to biomass, including tiller number, compared
347 to Nipponbare. Therefore, we investigated the source strength, sink features, sucrose
348 translocation as well as the fate of the photosynthates towards biomass and yield using
349 representative wild rice and cultivated variety, *O. sativa* cv. Nipponbare and *O. australiensis*,
350 respectively.
351
352 **Comparison of source efficiency and photosynthates utilization**
353 In order to compare source efficiency of the two selected accessions, we quantified
354 leaf photosynthesis rate and related physiological traits as well as soluble sugars/non-
355 structural carbohydrates (NSCs) content in leaves of the two accessions. A significant
356 difference in the leaf photosynthesis rate *A* was observed between the two species at booting,
357 and milk- and dough-stage of grain filling. Both the species showed increasing trend of leaf
358 photosynthesis from booting to milk stage, followed by reduction at the dough stage of grain
359 filling (Supplementary Fig. S3A). The higher photosynthesis in *O. australiensis* at the three
360 stages were also associated with higher g_sH_2O and *Ci* compared to Nipponbare
361 (Supplementary Fig. S3B, C). Next, we measured the different soluble sugars/NSCs, such as
362 sucrose, fructose, glucose and starch, at the time of photosynthesis quantification in leaves at
363 the milk stage of grain filling to evaluate the levels of primary carbon metabolites, the major
364 outcome of photosynthesis. The abundance of all four NSCs were significantly higher in the
365 leaves of *O. australiensis* than Nipponbare (Fig. 2A, B). Interestingly, *O. australiensis* also
366 accumulated higher levels of starch in leaves compared to Nipponbare, suggesting abundance
367 of residual sugar in the wild rice that is converted to starch. In contrast, the starch content was
368 found to be significantly lower in *O. australiensis* grains compared to Nipponbare, despite
369 starch being the major reserve product of seeds (Fig. 2C). Higher starch and soluble sugar
370 content in *O. australiensis* leaf and lower starch levels in seed suggested possible bottlenecks
371 in the mobilization of photosynthates to grains in the wild rice.
372 We, then, quantified end of the day (EOD) and end of the night (EON) carbon status
373 in the leaves of the two accessions. Glucose and fructose level were significantly lower in *O.*

374 *australiensis* than *O. sativa* cv. Nipponbare at the EOD and EON (Supplementary Fig. S4A).
375 Sucrose content was marginally, but significantly, higher in *O. australiensis* compared to *O.*
376 *sativa* cv. Nipponbare at the EOD as well as EON. At the EOD, *O. australiensis* accumulated
377 more starch in leaves than *O. sativa* cv. Nipponbare (Supplementary Fig. S4B). However, *O.*
378 *australiensis* displayed a significantly lower leaf starch level than *O. sativa* cv. Nipponbare at
379 the EON, suggesting efficient utilization of stored starch in *O. australiensis* during the night
380 (Supplementary Fig. S4B). This is in contrast to lower starch content in the grains of *O.*
381 *australiensis* as explained earlier (Fig. 2C). These results clearly indicated the efficient
382 utilization of the photosynthates in the wild rice, however not towards grain filling,
383 suggesting the possibility of the alternative sink and alternative fate of photosynthates.
384
385 **Phloem loading and export of sucrose from leaves**
386 Since sucrose is the major transportable form of photosynthates from source leaves to
387 sink organs, we investigated the sucrose transport differences between the two accessions.
388 We performed [^{14}C] labelled sucrose assay in leaf discs of *O. sativa* cv. Nipponbare and *O.*
389 *australiensis*. The higher amount of ^{14}C per unit leaf disc area was detected *O. australiensis*
390 (5598.83 CPM per cm^2) compared to that of in Nipponbare (3446.66 CPM per cm^2) (Fig.
391 2D). We, then, quantified sucrose in the phloem sap of the two accessions. Phloem sap of *O.*
392 *australiensis* had four times higher sucrose content than *O. sativa* cv. Nipponbare (Fig. 2E).
393 Together, ^{14}C-assay and analysis of phloem sap showed the efficient phloem loading and
394 sucrose export from the leaf in the wild rice *O. australiensis* compared to Nipponbare.
395
396 **Expression pattern of genes encoding sucrose transporters**
397 We examined the contribution of sucrose transporters for differences in phloem
398 loading and sucrose export from leaves. Transcript levels of genes encoding clade III SWEET
399 transporters, as well as SUT transporters were quantified. Expression analysis of *OsSWEET*s
400 using publicly available datasets showed preferentially source-specific expression of
401 *OsSWEET13* (Supplementary Fig. S5A). *OsSWEET14* also followed a similar source-specific
402 expression pattern, but at a relatively lower expression level than *OsSWEET13*. *OsSWEET15*
403 and *OsSWEET11* showed preferentially sink (panicle and endosperm) specific expression
404 patterns. The expression levels of *OsSWEET12* was observed to be very low in all the tissues.
405 Consistent with this, quantitative Real Time-PCR results showed higher transcript levels of
406 *OsSWEET13* in flag leaf and stem; *OsSWEET11* in the spikelet; and *OsSWEET15* in the stem,
407 spikelet, and flag leaf of Nipponbare (Fig. 3A-D). Interestingly, the transcript level of

408 *OsSWEET13*, encoding preferentially source-specific SWEET transporter, was significantly
409 higher in flag leaf and stem of *O. australiensis* compared to Nipponbare (Fig. 3A, B). *In*
410 *silico* expression analysis showed higher expression of *OsSUT1* and *OsSUT2* in different
411 tissue compared to other *OsSUT*s (Supplementary Fig. S5B). qRT-PCR analysis confirmed
412 the generally higher expression of *OsSUT1* and *OsSUT2* in different tissues of Nipponbare
413 (Fig. 3E-H). We detected higher transcript levels of *OsSUT1* in the flag leaf, and *OsSUT2* in
414 the stem of *O. australiensis* compared to Nipponbare (Fig. 3E, F). The expression pattern of
415 *OsSWEET*s and *OsSUT*s suggested the potential involvement of selected SWEET and SUT
416 transporters, such as OsSWEET13, OsSUT1, and OsSUT2, in efficient phloem loading and
417 sucrose export from leaf to stem in the wild rice.
418 Despite higher photosynthetic efficiency and efficient sucrose transport from source
419 leaves, *O. australiensis* produced smaller and lighter grains with less starch content compared
420 to the cultivated variety Nipponbare. Therefore, we also examined the transcript levels of
421 different sucrose transporters in developing spikelets. The expression levels of all the
422 *OsSWEET*s were significantly lower in spikelets of *O. australiensis* compared to Nipponbare,
423 with almost no expression of preferentially sink-specific *OsSWEET15* and *OsSWEET11* (Fig.
424 3D). In addition, the transcript levels of *OsSUT1* was significantly lower in developing
425 spikelet of *O. australiensis* than Nipponbare (Fig. 3H). Thus, reduced grain filling in *O.*
426 *australiensis* could potentially be associated with reduced expression of *OsSWEET15*,
427 *OsSWEET11*, and *OsSUT1*.
428
429 **Differences in vascular features associated with sucrose transport**
430 Vascular features are also key to photoassimilate partitioning from source to sink
431 tissues. Therefore, we quantified the vein number and vein width in the fully matured flag
432 leaves of the two accessions. *O. australiensis* leaves had a greater number of wider veins
433 compared to Nipponbare (Fig. 4A, B). Moreover, *O. australiensis* also exhibited higher vein
434 density with lesser interveinal distance compared to Nipponbare (Supplementary Fig. S6A,
435 B). We, then, checked the organization of vascular bundles at the panicle base of the two
436 accessions, as panicle base is the site of attachment of spikelets to the main plant (Zhang *et*
437 *al.,* 2002; Zhai *et al.,* 2018). *O. australiensis* had a fewer number of vascular bundles with the
438 reduced area than Nipponbare at the panicle base (Fig. 4C, D). We also quantified the
439 vascular features in the stem of the two accessions (Fig. 4E, F). Interestingly, we observed
440 ~1.7 times larger vascular bundles in the *O. australiensis* stem compared to Nipponbare.

441 Further, *O. australiensis* stem also had approximately twice the number of vascular bundles
442 than Nipponbare stem due to wider stem (Fig. 4F). Taken together, the sucrose might not be
443 efficiently mobilized to panicle in *O. australiensis*, likely due to defects in the vascular
444 bundle at the panicle base and minimal expression of *OsSWEET*s in developing spikelets,
445 strengthening the hypothesis of alternative utilization of photosynthates in the *O.*
446 *australiensis* stem towards higher biomass.
447
448 **Starch accumulation and expression levels of starch-biosynthesis genes in stem**
449 The leaf photosynthesis, efficient phloem loading in leaves, vascular features as well
450 as the expression pattern of sucrose transporter genes indicated stem to be a major sink organ
451 utilizing sucrose received from leaves in *O. australiensis*. Therefore, we quantified the
452 content of NSCs in stems of the two species at milk-stage of grain filling (Fig. 5A, B).
453 Significantly lower amounts of glucose, fructose and sucrose were detected in the stem of *O.*
454 *australiensis* as compared to Nipponbare (Fig. 5A). This was in contrast to more amount of
455 sucrose being exported from leaves of *O. australiensis*. Therefore, we suspected that *O.*
456 *australiensis* might reserve a high amount of starch in their stem. To our surprise, a negligible
457 amount of starch was present in the stem of *O. australiensis* compared to Nipponbare (Fig.
458 5B). Starch content was, further, found to be very low in the *O. australiensis* stems at
459 different stages and in different internodes (Fig. S7A, B). We, then, checked the expression
460 of key genes involved in starch biosynthesis, *OsAPL3*, *OsAPS1* and *OsSSIIb.* Expectedly,
461 very high expressions of these genes were detected in internode and stem of the cultivated
462 variety Nipponbare by both *in silico* expression analysis as well as qRT-PCR analysis (Fig.
463 5C; Supplementary Fig. S8A). Consistent with very low starch levels in *O. australiensis* stem
464 and internode, the transcript abundance of genes encoding two key enzymes, *OsAPL3* and
465 *OsAPS1*, was drastically less in *O. australiensis* compared to Nipponbare (Fig. 5C). Lower
466 amount of soluble non-structural carbohydrates, in particular remarkably low starch content,
467 despite efficient sucrose transport from leaves to stem, confirmed an alternative fate to
468 photosynthates in *O. australiensis* stem.
469
470 **Expression levels of sucrose metabolism genes, Sucrose Synthase enzyme activity, and**
471 **structural carbohydrate levels in stem**
472 Invertases (INV) and Sucrose Synthase (SUS) are the key enzymes for degradation of
473 sucrose. Expression of genes encoding Invertases have been shown to be strongly correlated
474 with starch synthesis (Ruan, 2014; Bahaji *et al.*, 2014). Therefore, we checked the expression

475 pattern of different genes encoding cell wall Invertase (*OsCIN1*), cytoplasmic Invertase
476 (*OsNIN7*), and vacuolar Invertase (*OsINV2*) (Supplementary Fig. S9). The expression of
477 *OsCIN1* was drastically lower in *O. australiensis* indicating limited breakdown of sucrose
478 that remained in stem apoplast during the transport.

479 Among all the *OsSUS*s, *OsSUS1* was shown to be highly expressed in internodes
480 (Hirose *et al.*, 2008). *In silico* expression analysis also showed high expression of *OsSUS1* in
481 internodes (Fig. S8A). Therefore, we checked the intracellular localization of OsSUS1 and
482 expression levels of the corresponding gene. The OsSUS1-YFP signal overlapped with the
483 plasma membrane-localized marker (PM-mCherry), confirming OsSUS1 localization in
484 plasma membrane (Supplementary Fig. S10). *OsSUS1* was expressed four times higher in *O.*
485 *australiensis* stem than Nipponbare, indicating a possibility of cellulose accumulation in *O.*
486 *australiensis* stem (Fig. 6A). Since SUS catalyzes a reversible cleavage of sucrose, it has a
487 synthesis activity promoting sucrose synthesis and a cleavage activity promoting sucrose
488 degradation. The enzyme activity assay revealed higher OsSUS1 synthesis activity in
489 Nipponbare, while higher cleavage activity in *O. australiensis* (Fig. 6B, C). Lesser
490 accumulation of starch, more transcript levels of *OsSUS1*, and higher cleavage activity of
491 OsSUS1 in *O. australiensis* stem compared to Nipponbare along with localization of OsSUS1
492 to plasma membrane prompted us to check the cellulose content in the stems of the two
493 accessions. Cellulose synthase genes are usually expressed at the highest levels in rice
494 internodes compared to other tissues as evident from *in silico* expression analysis (Fig. S8B).
495 Interestingly, transcript levels of *OsCES4*, *OsCES7*, and *OsCES9*, key cellulose synthesis
496 genes, were significantly higher in the stems of *O. australiensis* than in Nipponbare (Fig.
497 6D). Calcofluor-white staining along with cellulose quantification confirmed more cellulose
498 deposition in *O. australiensis* stem compared to Nipponbare (Fig. 6E, F). Like cellulose,
499 hemicellulose content was also significantly higher in *O. australiensis* stem compared to
500 Nipponbare (Fig. 6F). Taken together, higher expression of *OsSUS1* and higher cleavage
501 activity of OsSUS1 coupled with higher expression of Cellulose Synthase genes, at least in
502 part, led to efficient utilization of photosynthates in the *O. australiensis* stem.
503

504 **Discussion**

505 We investigated the differences in source-sink dynamics between a cultivated rice
506 variety *O. sativa* cv. Nipponbare, which is optimized for high grain yield, and a wild relative
507 of rice *O. australiensis*, which accumulates high biomass with poor grain yield. *O.*
508 *australiensis* had higher source strength, as evident by consistently higher leaf photosynthesis

509 rate compared to Nipponbare, at least in part due to vascular features of the leaf
510 (Supplementary Fig. S3A and Fig.4A, B). High leaf photosynthesis, usually, results in high
511 biomass or yield depending upon preferential sink tissues, provided efficient transport of
512 photoassimilates from leaves (Burnett *et al.*, 2016; Fabre *et al.*, 2020; Fernie *et al.*, 2020).
513 Limitations in sucrose export accumulate sugars in leaves, thereby inhibiting leaf
514 photosynthesis. Therefore, an efficient sucrose export system from leaf would be warranted
515 for the realization of higher source strength of the wild rice to high biomass and/or yield. ^{14}C
516 sucrose uptake assay, as well as sucrose content in phloem sap, confirmed the efficient
517 sucrose export from wild rice leaves (Fig. 2D, E). Larger vascular bundles and fewer number
518 of mesophyll cells between two consecutive veins potentially mediated efficient sucrose
519 export from leaves in wild rice, as reported in different plant system (Qi *et al.*, 2008; Fujita *et*
520 *al.*, 2013; Mathan *et al.*, 2016). In addition, higher expression of genes encoding sucrose
521 transporters, OsSWEET13 and OsSUT1, would also facilitate the efficient phloem loading in
522 the wild rice (Fig. 3). High expression of *SbSWEET8-1* of sorghum, a close homolog of
523 *OsSWEET13*, in leaf and its function in phloem loading supports our idea of the important
524 role of *OsSWEET13* for phloem loading (Mizuno *et al.,* 2016). Similarly, *OsSUT1* not only
525 functions for enhancing phloem loading for sucrose transport but also for retrieval of sucrose
526 from the apoplasm along the transport pathway (Scofield *et al.*, 2007). Higher amount of
527 soluble sugars in wild rice leaves, despite having higher sucrose export from leaves,
528 compared to the cultivated variety, further supported the better source strength of the wild
529 rice (Fig. 2 A, B).

530 The better grain filling and higher grain yield of cultivated rice, despite of the
531 relatively lower source strength compared to *O. australiensis*, could be explained by optimal
532 vascular features and desirable expression sucrose transporter genes at the panicle base and
533 spikelets of cultivated rice (Fig. 3, 4). Panicle architecture, a key determinant of rice grain
534 yield, is reported to be shaped by the vascular pattern (Sasahara *et al.*, 1999; Terao *et al.*,
535 2010). Reduced expression of *OsSWEET13* and *OsSWEET15* in the developing spikelet, and
536 of *OsSUT1* at the panicle base and developing spikelet, along with reduced supply of smaller
537 vascular bundles at the panicle base limited mobilization of photosynthates to grains in the
538 wild rice compared to the cultivated. In agreement with this, *ossweet11 ossweet15* double
539 mutant has been reported to show smaller seed size (Yang *et al.*, 2018). Similarly, RNA
540 antisense lines of *OsSUT1* showed reduced grain filling and grain weight (Scofield *et al.*,
541 2007). Increased supply of larger vascular bundles to rice rachis has been shown to promote
542 more grains per panicle (Zhang *et al.*, 2002; Terao *et al.*, 2010; Zhai *et al.*, 2018). Altogether,

543 higher source strength and limited grain sink strength in the wild rice, attributed to vascular
544 features and sucrose transporter functions, indicated preferential utilization of photosynthates
545 in stem and internodes, contributing to source-sink relationship differences between the
546 selected cultivated and wild rice. In conjunction with this, larger vascular bundles would
547 facilitate efficient sucrose transport and unloading in the wild rice stem. Such vascular
548 features in the stem would, in turn, also provide mechanical strength to support the high
549 biomass of the wild rice (Aohara *et al.*, 2009). Our expression results indicated the potential
550 involvement of OsSWEET13 and OsSUT2 in unloading larger amount of sucrose being
551 received in the wild stem.

552 There is a competition among the sink tissues for utilization of photosynthates
553 (Patrick *et al.*, 2013; Durand *et al.*, 2018). According to the EcoMeristem model, the final
554 plant architecture is an outcome of competition for resources among different plant parts that
555 depends on photoassimilate-partitioning patterns (Luquet *et al.*, 2006). More number of
556 longer internodes and thicker stem with larger leaves, driving high biomass in the wild rice
557 compared to the cultivated variety, suggested higher utilization of photosynthates for
558 vegetative growth. The higher biomass and larger organ size of wild rice would require more
559 photosynthates for general respiration and maintenance. However, this would likely not
560 explain the utilization of photosynthates in total as wild rice showed remarkably higher
561 amount of sucrose in phloem sap compared to the cultivated variety. Altogether, wild rice
562 efficiently utilized photoassimilates reaching to stem towards larger vegetative organ size and
563 number, cell-wall thickening as well as the overall maintenance of higher biomass as
564 compared to the cultivated rice variety.

565 The preferential utilization of photosynthates in the stem/internodes of wild rice in
566 contrast to grains in the cultivated rice suggested differences in the photosynthates
567 metabolism in the stem of the two species. Cultivated rice variety clearly accumulated higher
568 starch content in the stem, which is mobilized to panicle during grain filling (Fig. 5B).
569 *OsSWEET11* and *OsSWEET15* have been suggested to be important for remobilization of
570 carbon reserve from stem to grain, and OsSUT1 in the retrieval of sucrose from apoplasmic
571 space to stem for conversion to transitory starch (Wang *et al.*, 2020). Indeed, Nipponbare
572 stem showed higher expression of *OsSWEET11*, *OsSWEET15*, and *OsSUT1* compared to the
573 wild rice along with desirable vascular features at the panicle base. High expression of starch
574 biosynthesis genes, further, contributed to the roles of the stem as an effective source in the
575 cultivated variety at the grain filling stage (Fig. 7). The differences in the stem starch content

576 between the two genotypes projected the stored transitory starch in the stem as a key for
577 source-sink dynamics favoring high grain yield.

578 *O. australiensis* stem showed higher expression of *OsSUS1* and higher cleavage
579 activity OsSUS producing higher amount of UDP-glucose and fructose compared to
580 cultivated rice. UDP-glucose has been shown to serve as the prime source for cellulose
581 synthesis (Smith *et al*., 2012). UDP-glucose can possibly also be converted to starch (Asano
582 *et al*., 2002; Koch, 2004). However, the possibility is minimized in the wild rice due to very
583 limited expression of *OsAPL3* and *OsAPS1*. Thus, most of the SUS-generated UDP-glucose
584 was converted to cellulose, supported by high expression of cellulose synthase genes,
585 *OsCES4*, *OsCES7*, and *OsCES9* in the wild stem (Fig. 6D-F). OsSUS1 has been reported to
586 be located in SE-CC complexes of phloem, and localization of SUS in phloem is important
587 for cellulose synthesis (Smith *et al*., 2012; Regmi *et al.*, 2016). Plasma membrane
588 localization of OsSUS1 in this study together with earlier reported association of cellulose
589 synthase complexes to plasma membrane highlighted the key importance of OsSUS1 for
590 cellulose synthesis in rice (Supplementary Fig. S10, Lei *et al*., 2012). In addition, SUS
591 functions in companion cells of phloem has been suggested to enhance the sucrose unloading
592 at sink tissues, further helping in unloading photosynthates in wild rice stem (Nolte and
593 Koch, 1993; Stein and Granot, 2019, Yao *et al.*, 2020). The potential role of SUS in cellulose
594 synthesis, as well as in secondary cell wall thickening, has been investigated in the past
595 (Coleman *et al.*, 2009; Baroja-Fernández *et al.*, 2012; Wei *et al.*, 2015). Consistent with the
596 higher expression of *OsSUS1* in wild rice, overexpression of *SUS* has been shown to result in
597 increased vegetative growth rate, plant height and biomass in different plant species
598 (Coleman *et al.*, 2006; Nguyen *et al.*, 2016; Stein and Granot, 2019). Contrary to the wild
599 rice, higher synthesis activity of OsSUS in Nipponbare stem would facilitate the formation of
600 sucrose from the stored starch at the heading stage to be mobilized for grain filling. Thus,
601 differential functions in OsSUS1 between wild and cultivated rice would, at least in part,
602 explain the differential fate of photosynthates in the stem (Fig. 7).

603 In summary, differences in vascular features and sucrose transporter functions led to a
604 differential source-sink relationship between wild rice *O. australiensis* and cultivated variety
605 *O. sativa* cv. *Nipponbare*. Wild rice showed source-sink dynamics favoring high biomass
606 through accumulation of structural carbohydrates, mediated by higher cleavage activity of
607 SUS enzyme together with higher expression of Cellulose Synthase genes (Fig. 7). In
608 contrast, source-sink dynamics favored higher grain yield in Nipponbare via accumulation of
609 transitory starch in the stem, to be mobilized to panicles with the onset of grain filling. Taken

610 together, vascular features and sucrose transporter functions along with transitory starch
611 storage mechanism and SUS enzyme activity can potentially be targeted for source-sink
612 dynamics favoring either biomass accumulation in fodder crops or higher grain yield in cereal
613 crops.
614
615 **Supplementary data**
616 Fig. S1. Biomass and yield-related traits of the selected cultivated and wild rice genotypes.
617
618 Fig. S2. Principal component analysis of biomass and seed traits of the selected cultivated
619 and wild rice species.
620
621 Fig. S3. Leaf photosynthesis and related physiological differences between the cultivated rice
622 *O. sativa* cv. Nipponbare and wild rice *O. australiensis*.
623
624 Fig. S4. Sugar content in leaves of cultivated rice *O. sativa* cv. Nipponbare and wild rice *O.*
625 *australiensis* at End of Day (EOD) and End of Night (EON).
626
627 Fig. S5. *In silico* organ-specific expression analysis of rice genes encoding SWEET and SUT
628 transporters.
629
630 Fig. S6. Quantification of leaf interveinal distance and vein density for cultivated rice *O.*
631 *sativa* cv. Nipponbare and wild rice *O. australiensis*.
632
633 Fig. S7. Total starch content in stem and internodes of cultivated rice *O. sativa* cv.
634 Nipponbare and wild rice *O. australiensis*.
635
636 Fig. S8. *In silico* expression pattern of key genes involved in sugar metabolism in rice.
637
638 Fig. S9. Transcript levels of genes encoding cell wall invertase (*OsCIN1*), cytoplasmic
639 invertase (*OsNIN7*), and vacuolar invertase (*OsINV2*).
640
641 Fig. S10. Localization of OsSUS1-YFP in plasma membrane.
642
643 Table S1. List of primer pairs used in the study

Acknowledgements

This work was supported by the Innovative Young Biotechnologist Award (BT/09/IYBA/2015/01) and Ramalingaswamy Re-entry Fellowship (BT/RLF/reentry/05/2013) to AR from the Department of Biotechnology, Ministry of Science and Technology, India. JM and AS acknowledge their CSIR-JRF and SERB-NPDF fellowships, respectively. We also acknowledge Central Instrument Facility, NIPGR; Advanced Instrumentation Research Facility, JNU; Confocal Microscopy Facility, NIPGR; and DBT-eLibrary Consortium (DeLCON) for providing access to e-resources.

Author Contributions

JM and AR conceptualized the study and designed experiments. JM performed experiments. JM and AS analysed data. JM, AS and AR wrote the manuscript. All the authors have read and edited the final manuscript.

Data availability statement

Data sharing is not applicable to this article as all created data is already contained within this article or in the supplementary material.

References

Ambavaram, M.M.R., Krishnan, A., Trijatmiko, K.R. and Pereira, A. 2011. Coordinated activation of cellulose and repression of lignin biosynthesis pathways in rice. Plant Physiology **155,** 916–931.

Asano, T., Kunieda, N., Omura, Y., et al. 2002. Rice SPK, a calmodulin-like domain protein kinase, is required for storage product accumulation during seed development: Phosphorylation of sucrose synthase is a possible factor. Plant Cell **14,** 619–628.

Aohara T, Kotake T, Kaneko Y, Takatsuji H, Tsumuraya Y, Kawasaki S. 2009. Rice brittle culm 5 (brittle node) is involved in secondary cell wall formation in the sclerenchyma tissue of nodes. Plant and Cell Physiology **50**, 1886–1897.

Bahaji A, Li J, Sánchez-López ÁM, *et al.* 2014. Starch biosynthesis, its regulation and biotechnological approaches to improve crop yields. Biotechnology Advances **32**, 87–106.

Baroja-Fernández E, Muñoz FJ, Li J, Bahaji A, Almagro G, Montero M, Etxeberria E, Hidalgo M, Sesma MT, Pozueta-Romero J. 2012. Sucrose synthase activity in the sus1/sus2/sus3/sus4 Arabidopsis mutant is sufficient to support normal cellulose and starch production. Proceedings of the National Academy of Sciences of the United States of America **109**, 321–326.

Braun DM. 2012. Sweet! The pathway is complete. Science **335**, 173–174.

Burnett AC, Rogers A, Rees M, Osborne CP. 2016. Carbon source–sink limitations differ between two species with contrasting growth strategies. Plant Cell and Environment **39**, 2460–2472.

Chen LQ, Qu XQ, Hou BH, Sosso D, Osorio S, Fernie AR, Frommer WB. 2012. Sucrose efflux mediated by SWEET proteins as a key step for phloem transport. Science **335**, 207–211.

Cho J Il, Kim HB, Kim CY, Hahn TR, Jeon JS. 2011. Identification and characterization of the duplicate rice sucrose synthase genes OsSUS5 and OsSUS7 which are associated with the plasma membrane. Molecules and Cells **31**, 553–561.

Coleman HD, Ellis DD, Gilbert M, Mansfield SD. 2006. Up-regulation of sucrose synthase and UDP-glucose pyrophosphorylase impacts plant growth and metabolism. Plant Biotechnology Journal **4**, 87–101.

Coleman, H.D., Yan, J. and Mansfield, S.D. 2009. Sucrose synthase affects carbon partitioning to increase cellulose production and altered cell wall ultrastructure. Proceedings of the National Academy of Sciences of the United States of America **106**, 13118–13123.

Durand M, Mainson D, Porcheron B, Maurousset L, Lemoine R, Pourtau N. 2018. Carbon source–sink relationship in Arabidopsis thaliana: the role of sucrose transporters. Planta **247**, 587–611.

Earley KW, Haag JR, Pontes O, Opper K, Juehne T, Song K, Pikaard CS. 2006. Gateway-compatible vectors for plant functional genomics and proteomics. The Plant Journal **45**, 616–629.

Fabre D, Dingkuhn M, Yin X, Clément-Vidal A, Roques S, Soutiras A, Luquet D. 2020. Genotypic variation in source and sink traits affects the response of photosynthesis and growth to elevated atmospheric CO2. Plant Cell and Environment **43**, 579–593.

Fan C, Feng S, Huang J, *et al.* 2017. AtCesA8-driven OsSUS3 expression leads to largely enhanced biomass saccharification and lodging resistance by distinctively altering lignocellulose features in rice. Biotechnology for Biofuels **10**, 1–12.

Fernie AR, Bachem CWB, Helariutta Y, *et al.* 2020. Metabolic Aspects of Source – Sink Interactions. Nature Plants **6**.

Fujita D, Trijatmiko KR, Tagle AG, *et al.* 2013. NAL1 allele from a rice landrace greatly increases yield in modern indica cultivars. Proceedings of the National Academy of Sciences of the United States of America **110**, 20431–20436.

Guevara DR, El-Kereamy A, Yaish MW, Mei-Bi Y, Rothstein SJ. 2014. Functional characterization of the rice UDP-glucose 4-epimerase 1, OsUGE1: A potential role in cell wall carbohydrate partitioning during limiting nitrogen conditions. PLoS ONE **9**.

Haigler CH, Ivanova-Datcheva M, Hogan PS, Salnikov V V., Hwang S, Martin K, Delmer DP. 2001. Carbon partitioning to cellulose synthesis. Plant Molecular Biology **47**,

29–51.

Hirose T, Scofield GN, Terao T. 2008. An expression analysis profile for the entire sucrose synthase gene family in rice. Plant Science **174**, 534–543.

Julius BT, Leach KA, Tran TM, Mertz RA, Braun DM. 2017. Sugar transporters in plants: New insights and discoveries. Plant and Cell Physiology **58**, 1442–1460.

King, R.W. and Zeevaart, J.A.D. 1974. Enhancement of Phloem Exudation from Cut Petioles by Chelating Agents. Plant Physiol*o*gy **53**, 96–103.

Koch, K. 2004. Sucrose metabolism: Regulatory mechanisms and pivotal roles in sugar sensing and plant development. Current Opinion in Plant Biology **7**, 235–246.

Lei, L., Li, S., and Gu, Y. 2012. Cellulose synthase complexes: composition and regulation. Frontiers in plant science **3**, 75.

Lisec J, Schauer N, Kopka J, Willmitzer L, Fernie AR. 2006. Gas chromatography mass spectrometry-based metabolite profiling in plants. Nature Protocols **1**, 387–396.

Livak KJ, Schmittgen TD. 2001. Analysis of relative gene expression data using real-time quantitative PCR and the 2-ΔΔCT method. Methods **25**, 402–408.

Luquet D, Dingkuhn M, Kim H, Tambour L, Clement-Vidal A. 2006. EcoMeristem, a model of morphogenesis and competition among sinks in rice. 1. Concept, validation and sensitivity analysis. Functional Plant Biology **33**, 309–323.

Mathan J, Bhattacharya J, Ranjan A. 2016. Enhancing crop yield by optimizing plant developmental features. Development (Cambridge) **143**, 3283-3294.

Mitra, P.P. and Loqué, D. 2014. Histochemical staining of Arabidopsis thaliana secondary cell wall elements. Journal of Visualized Experiments **13**, 51381.

Mizuno, H., Kasuga, S. and Kawahigashi, H. 2016. The sorghum *SWEET* gene family: stem sucrose accumulation as revealed through transcriptome profiling. Biotechnology for Biofuels **9,** 127.

Mund, N.K., Dash, D., Barik, C.R., Goud, V. V., Sahoo, L., Mishra, P. and Nayak, N.R. 2016. Chemical composition, pretreatments and saccharification of Senna siamea (Lam.) H.S.

Irwin & Barneby: An efficient biomass producing tree legume. Bioresource Technology **207**, 205–212.

Nelson, B.K., Cai, X. and Nebenführ, A. 2007. A multicolored set of in vivo organelle markers for co-localization studies in Arabidopsis and other plants. Plant Journal **51**, 1126–1136.

Nguyen QA, Luan S, Wi SG, Bae H, Lee DS, Bae HJ. 2016. Pronounced phenotypic changes in transgenic tobacco plants overexpressing sucrose synthase may reveal a novel sugar signaling pathway. Frontiers in Plant Science **6**, 1216.

Nolte KD, Koch KE. 1993. Companion-cell specific localization of sucrose synthase in zones of phloem loading and unloading. Plant Physiology **101**, 899–905.

Osorio S, Ruan YL, Fernie AR. 2014. An update on source-to-sink carbon partitioning in tomato. Frontiers in Plant Science **5**, 1–11.

Patrick JW, Botha FC, Birch RG. 2013. Metabolic engineering of sugars and simple sugar derivatives in plants. Plant Biotechnology Journal **11**, 142–156.

Qazi, H.A., Paranjpe, S. and Bhargava, S. 2012. Stem sugar accumulation in sweet sorghum - Activity and expression of sucrose metabolizing enzymes and sucrose transporters. Journal of Plant Physiology **169**, 605–613.

Qi J, Qian Q, Bu Q, *et al.* 2008. Mutation of the rice narrow leaf1 gene, which encodes a novel protein, affects vein patterning and polar auxin transport. Plant Physiology **147**, 1947–1959.

Regmi KC, Zhang S, Gaxiola RA. 2016. Apoplasmic loading in the rice phloem supported by the presence of sucrose synthase and plasma membrane-localized proton pyrophosphatase. Annals of Botany **117**, 257–268.

Ruan Y-L. 2014. Sucrose Metabolism: Gateway to Diverse Carbon Use and Sugar Signaling. Annual Review of Plant Biology **65**, 33–67.

Sack L, Scoffoni C. 2013. Leaf venation : structure , function , development , evolution , ecology and applications in the past, present and future. New Phytologist **4**, 983–1000.

Sanchez, P.L., Wing, R.A. and Brar, D.S. 2013. The wild relative of rice: genomes and genomics. In *Genetics and genomics of rice* (Zhang, Q. and Wing, R.A., eds). Springer, pp. 10–25.

Sasahara H, Fukuta Y, Fukuyama T. 1999. Mapping of QTLs for Vascular Bundle System and Spike Morphology in Rice, Oryza satva L. Breeding Science **49**, 75–81.

Scofield GN, Hirose T, Aoki N, Furbank RT. 2007. Involvement of the sucrose transporter, OsSUT1, in the long-distance pathway for assimilate transport in rice. Journal of Experimental Botany **58**, 3155–3169.

Scofield GN, Hirose T, Gaudron JA, Upadhyaya NM, Ohsugi R, Furbank RT. 2002. Antisense suppression of the rice sucrose transporter gene, OsSUT1, leads to impaired grain filling and germination but does not affect photosynthesis. Functional Plant Biology **29**, 815–826.

Smith AM, Kruger NJ, Lunn JE. 2012. Source of sugar nucleotides for starch and cellulose synthesis. Proceedings of the National Academy of Sciences of the United States of America **109**, E776–E776.

Smith AM, Stitt M. 2007. Coordination of carbon supply and plant growth. Plant, Cell and Environment **30**, 1126–1149.

Smith, M.R., Rao, I.M. and Merchant, A. 2018. Source-sink relationships in crop plants and their influence on yield development and nutritional quality. Frontiers in Plant Science **871**, 1–10.

Stein O, Granot D. 2019. An overview of sucrose synthases in plants. Frontiers in Plant Science **10**, 1–14.

Tanaka K, Murata K, Yamazaki M, Onosato K, Miyao A, Hirochika H. 2003. Three distinct rice cellulose synthase catalytic subunit genes required for cellulose synthesis in the secondary wall. Plant Physiology **133**, 73–83.

Terao T, Nagata K, Morino K, Hirose T. 2010. A gene controlling the number of primary rachis branches also controls the vascular bundle formation and hence is responsible to increase the harvest index and grain yield in rice. Theoretical and Applied Genetics **120**, 875–

893.

Wang DR, Han R, Wolfrum EJ, McCouch SR. 2017. The buffering capacity of stems: genetic architecture of nonstructural carbohydrates in cultivated Asian rice, Oryza sativa. New Phytologist **215**, 658–671.

Wang G, Li H, Gong Y, Yang J, Yi Y, Zhang J, Ye N. 2020*a*. Expression profile of the carbon reserve remobilization from the source to sink in rice in response to soil drying during grain filling. Food and Energy Security **3**, 1–14.

Wang D, Qin Y, Fang J, Yuan S, Peng L, Zhao J, Li X. 2016*a*. A missense mutation in the zinc finger domain of OsCESA7 deleteriously affects cellulose biosynthesis and plant growth in rice. PLoS ONE **11**, 1–16.

Wei Z, Qu Z, Zhang L, Zhao S, Bi Z, Ji X, Wang X, Wei H. 2015. Overexpression of poplar xylem sucrose synthase in tobacco leads to a thickened cell wall and increased height. PLoS ONE **10**, 1–20.

White, A.C., Rogers, A., Rees, M. and Osborne, C.P. 2016. How can we make plants grow faster? A source-sink perspective on growth rate. Journal of Experimental **67**, 31–45.

Yadav, U., Khadilkar, A., Shaikh, M., Turgeon, R. and Ayre, B. (2017) Quantifying the Capacity of Phloem Loading in Leaf Disks with [^{14}C]Sucrose. Bio-Protocol **7**, 1–12.

Yang J, Luo D, Yang B, Frommer WB, Eom JS. 2018. SWEET11 and 15 as key players in seed filling in rice. New Phytologist **218**, 604–615.

Yao D, Gonzales-Vigil E, Mansfield SD. 2020. Arabidopsis sucrose synthase localization indicates a primary role in sucrose translocation in phloem. Journal of Experimental Botany **71**, 1858–1869.

Zhai L, Zheng T, Wang X, Wang Y, Chen K, Wang S, Wang Y, Xu J, Li Z. 2018. QTL mapping and candidate gene analysis of peduncle vascular bundle related traits in rice by genome-wide association study. Rice **11**, 13.

Zhang ZH, Li P, Wang LX, Tan CJ, Hu ZL, Zhu YG, Zhu LH 2002. Identification of quantitative trait loci (QTLs) for the characters of vascular bundles in peduncle related to indica -japonica differentiation in rice (*Oryza sativa L.*) Euphytica **128**, 279 –284.

Figure legends

Fig. 1. Comparison of biomass and yield-related traits of the selected cultivated and wild rice genotypes.

(A) Shown are the photographs of the selected rice genotypes at the reproductive stage (scale bar = 30 cm).

(B–I) Quantification of plant height (B), total leaves per plant (C), flag leaf width (D), total internode number per main stem (E), fresh weight (F), dry weight (G), spikelet per panicle (H), and 500-seed weight (I) of the selected rice genotypes. Significance of difference among the genotypes was calculated using One-Way ANOVA with Tukey's post-hoc test (n = 10 data point from different plants, $p < 0.05$).

Fig. 2. Sugar accumulation, phloem loading, and sucrose export from a leaf for the cultivated rice *O. sativa* cv. Nipponbare and wild rice *O. australiensis*.

(A) Shown are glucose, fructose and sucrose content in the flag leaves of the cultivated and wild rice at the time of photosynthesis quantification.

(B–C) Starch content in the flag leaves (B), and in the matured seeds (C) of the cultivated and wild rice.

(D) Uptake of [^{14}C] sucrose in the flag leaf discs of the two species expressed as counts per minute per square centimeter of leaf area.

(E) Sucrose quantification in the phloem sap of the two species.

Data represents the mean and standard error of mean (SE), and significance of difference between the genotype was calculated using student t-test (*$p < 0.05$, **$p < 0.01$, ***$p < 0.001$).

Fig. 3. Tissue-specific expression pattern of genes encoding SWEET and SUT transporters in cultivated rice *O. sativa* cv. Nipponbare and wild rice *O. australiensis*.

(A–D) Transcript levels of *SWEET* genes in the flag leaf (A), stem (B) panicle base (C), and spikelet (D) at the milk-stage of grain-filling in the two rice species.

(E–H) Transcript levels of *SUT* genes in the flag leaf (E), stem (F) panicle base (G), and spikelet (H) at the milk-stage of grain-filling in the two rice species.

Data represents the mean and standard error of mean (SE) from three biological replicate per genotype (n = 3). Significance of difference between the genotype was calculated using student t-test (*$p < 0.05$, **$p < 0.01$, ***$p < 0.001$).

Fig. 4. Vascular features in flag leaf, panicle base, and stem of cultivated rice *O. sativa* cv. Nipponbare and wild rice *O. australiensis*.

(A-B) Cross-sections of flag leaves of the two species (A, scale bar = 100 μm), and quantification of minor vein width and the total number of veins (B).

(C-D) Transverse sections at the panicle base (0.5 cm above panicle node) of the two species (C, scale bar = 250 μm), and quantification of number and area of vascular bundles (D).

(E-F) Transverse sections of stems of the two species (E, scale bar = 100 μm), and quantification of number and area of vascular bundles (F).

The peripheral concentric ring of the panicle base and stem is represented as outer ring, and the inner wider circle is represented as inner ring in figures.

Data represents the mean and standard error of mean (SE) from fifteen cross-section images collected from five different plants and significance difference between the genotype was based on student t-test (*$p < 0.05$, **$p < 0.01$, ***$p < 0.001$).

Fig. 5. Quantification of soluble sugars and expression pattern of starch-biosynthesis genes in stems of cultivated rice *O. sativa* cv. Nipponbare and wild rice *O. australiensis* at milk-stage of grain-filling.

(A-B) Glucose, fructose, and sucrose content (A), and total starch content (B) in the stem of the two species (n = 4).

(C) Transcript levels of starch-biosynthesis genes, *OsAPL3* (encoding ADP-glucose pyrophosphorylase large subunit), *OsAPS1* (encoding ADP-glucose pyrophosphorylase small subunit), and *OsSSIIB* (encoding Starch synthase), in the stem of the two species.

Data represents the mean and standard error of mean (SE), and significance difference between the genotype was calculated using student t-test (*$p < 0.05$, **$p < 0.01$, ***$p < 0.001$).

Fig. 6. Expression levels of sucrose metabolism genes, Sucrose Synthase enzyme activity, and structural carbohydrates levels in stem tissue of cultivated rice *O. sativa* cv. Nipponbare and wild rice *O. australiensis* at milk-stage of grain-filling.

(A) Transcript levels of *Sucrose Synthase* 1 (*OsSUS1*).

(B-C) OsSUS enzyme activity in synthesis (B) and cleavage (C) direction.

(D) Transcript levels of *Cellulose Synthase* genes, *OsCES4*, *OsCES7*, and *OsCES9*.

(E) Calcofluor-white staining for cellulose deposition in the transverse stem sections of the two species. Red arrowhead shows higher deposition of cellulose in *O. australiensis* stem. Scale bar represents 500 µm.

(F) Quantification of cellulose and hemicellulose in the stems of the two species.

Data in a- d and f represents the mean and standard error of mean (SE), and significance of difference between the genotype was calculated using student t-test (*$p < 0.05$, **$p < 0.01$, ***$p < 0.001$).

Fig. 7. A model explaining the contribution of sucrose transport, Sucrose Synthase activity, starch biosynthesis, and synthesis of structural carbohydrates towards yield and biomass differences between wild rice *O. australiensis* and cultivated rice *O. sativa* cv. Nipponbare.

High leaf photosynthesis rate coupled with higher expression of selected *OsSWEET* and *OsSUT* genes lead to efficient export of sucrose from leaf in *O. australiensis* compared to *O. sativa* cv. Nipponbare. Sucrose, after getting unloaded to stem due to functions of *OsSWEET13*, *OsSUT1*, and *OsSUT2*, gets converted to UDP-G more efficiently in the wild rice due to higher expression of *OsSUS1* and more cleavage activity of OsSUS compared to the cultivated rice. Higher expression of *OsCES4, OsCES7,* and *OsCES9*, then, leads to more synthesis of cellulose in the stem of the wild rice. In contrast, higher expression of starch-biosynthesis genes, *AGPase* (small and large subunit), leads to higher starch content in the stem of the cultivated rice. Higher synthesis activity of OsSUS along with more expression of *OsSWEET11* and *OsSWEET15* in the cultivated rice facilitate efficient remobilisation of sucrose from stem to panicles at the grain-filling stage. SUC, sucrose (yellow colour circle); F, fructose; G, glucose; UDP-G, UDP-glucose; ADP-G, ADP-glucose; *INV*, Invertase; cwINV, cell wall Invertase; SUS, Sucrose Synthase.

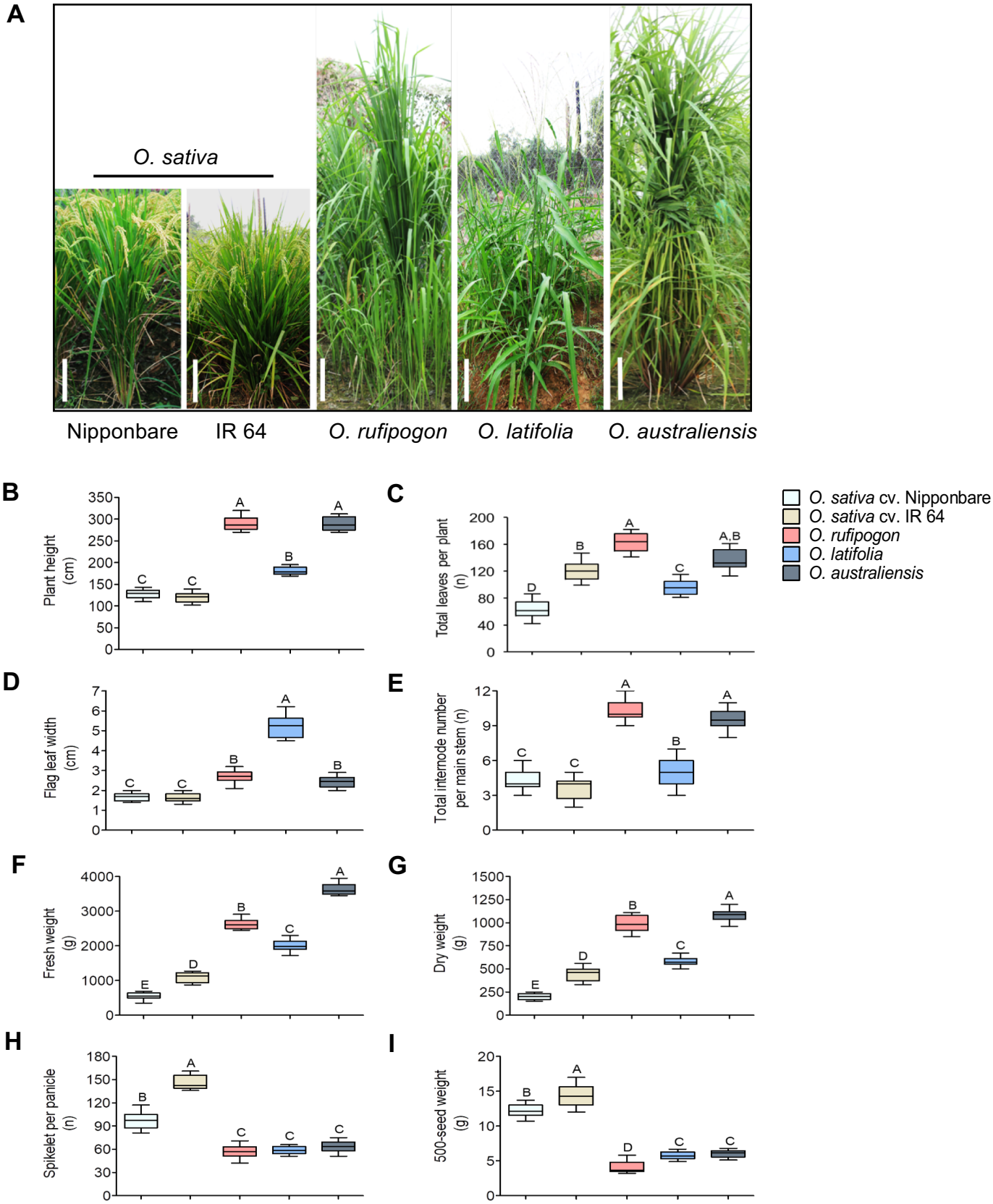

Fig. 1. Comparison of biomass and yield-related traits of the selected cultivated and wild rice genotypes.
(A) Shown are the photographs of the selected rice genotypes at the reproductive stage (scale bar = 30 cm).
(B–I) Quantification of plant height (B), total leaves per plant (C), flag leaf width (D), total internode number per main stem (E), fresh weight (F), dry weight (G), spikelet per panicle (H), and 500-seed weight (I) of the selected rice genotypes. Significance of difference among the genotypes was calculated using One-Way ANOVA with Tukey's post-hoc test (n = 10 data point from different plants, $p < 0.05$).

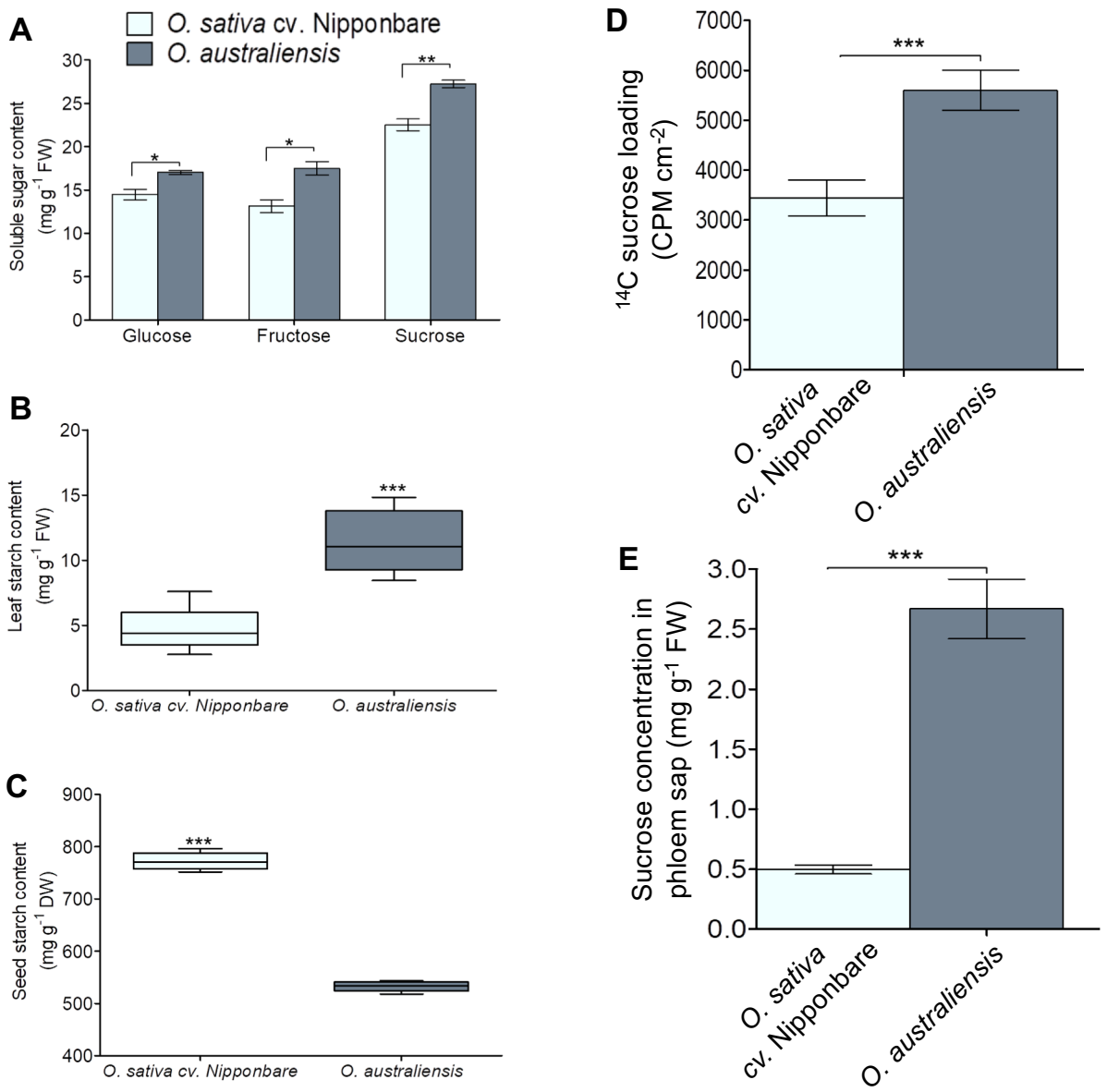

Fig. 2. Sugar accumulation, phloem loading, and sucrose export from a leaf for the cultivated rice *O. sativa* cv. Nipponbare and wild rice *O. australiensis*.

(A) Shown are glucose, fructose and sucrose content in the flag leaves of the cultivated and wild rice at the time of photosynthesis quantification.

(B–C) Starch content in the flag leaves (B), and in the matured seeds (C) of the cultivated and wild rice.

(D) Uptake of [^{14}C] sucrose in the flag leaf discs of the two species expressed as counts per minute per square centimeter of leaf area.

(E) Sucrose quantification in the phloem sap of the two species.

Data represents the mean and standard error of mean (SE), and significance of difference between the genotype was calculated using student t-test (*$p < 0.05$, **$p < 0.01$, ***$p < 0.001$).

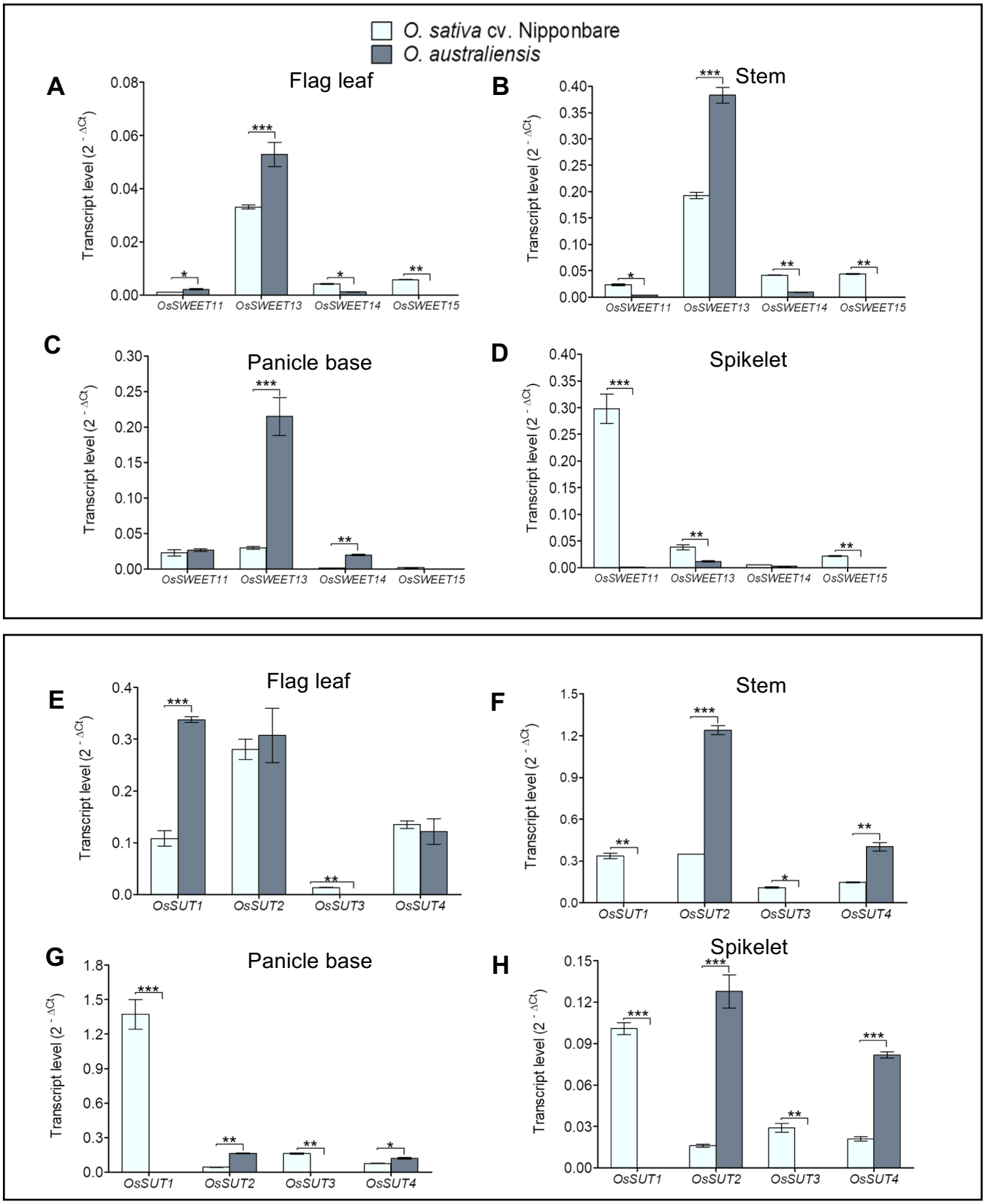

Fig. 3. Tissue-specific expression pattern of genes encoding SWEET and SUT transporters in cultivated rice *O. sativa* cv. Nipponbare and wild rice *O. australiensis*.

(A–D) Transcript levels of *SWEET* genes in the flag leaf (A), stem (B) panicle base (C), and spikelet (D) at the milk-stage of grain-filling in the two rice species.

(E–H) Transcript levels of *SUT* genes in the flag leaf (E), stem (F) panicle base (G), and spikelet (H) at the milk-stage of grain-filling in the two rice species.

Data represents the mean and standard error of mean (SE) from three biological replicate per genotype (n = 3). Significance of difference between the genotype was calculated using student t-test (*$p < 0.05$, **$p < 0.01$, ***$p < 0.001$).

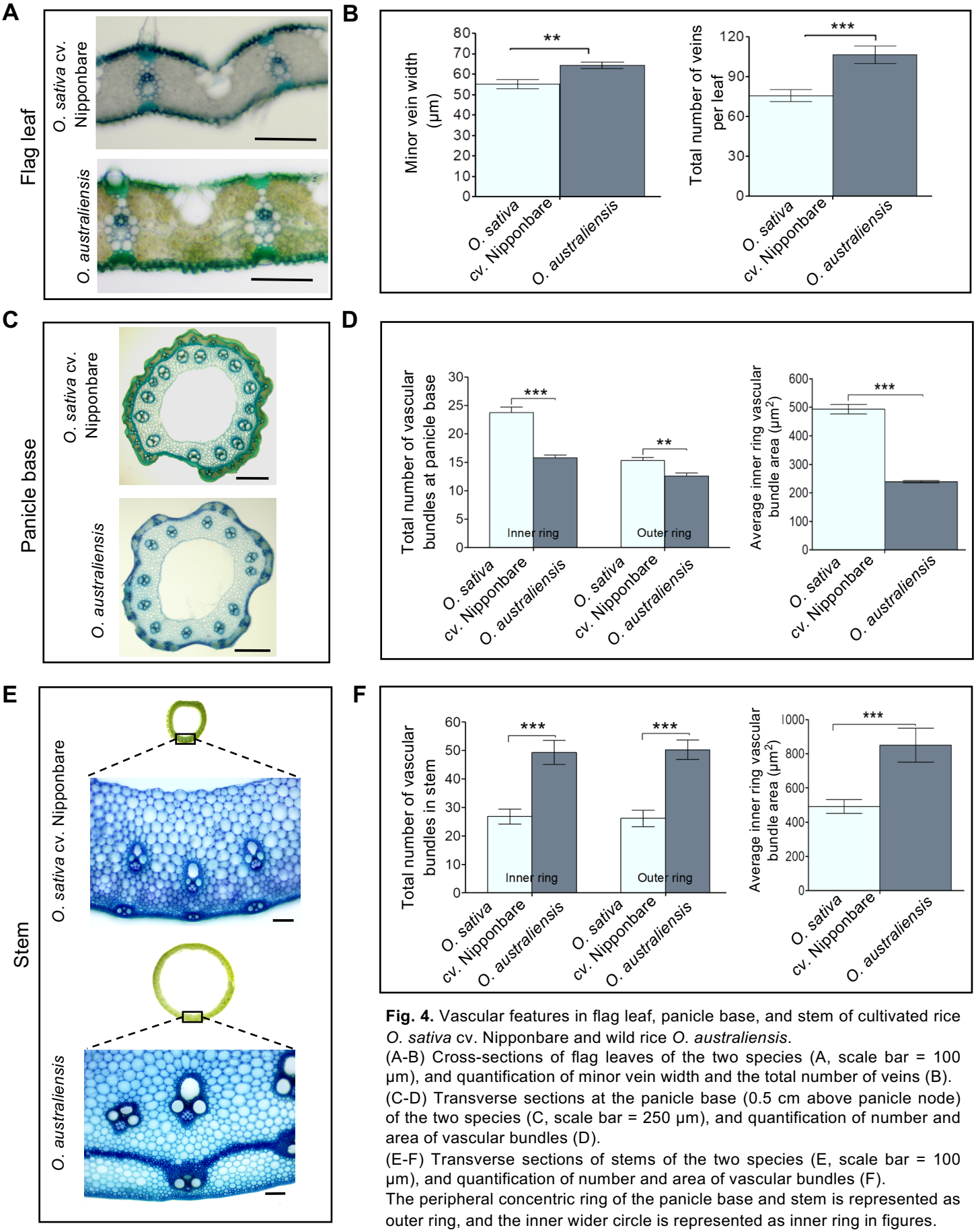

Fig. 4. Vascular features in flag leaf, panicle base, and stem of cultivated rice *O. sativa* cv. Nipponbare and wild rice *O. australiensis*.
(A-B) Cross-sections of flag leaves of the two species (A, scale bar = 100 µm), and quantification of minor vein width and the total number of veins (B).
(C-D) Transverse sections at the panicle base (0.5 cm above panicle node) of the two species (C, scale bar = 250 µm), and quantification of number and area of vascular bundles (D).
(E-F) Transverse sections of stems of the two species (E, scale bar = 100 µm), and quantification of number and area of vascular bundles (F).
The peripheral concentric ring of the panicle base and stem is represented as outer ring, and the inner wider circle is represented as inner ring in figures.
Data represents the mean and standard error of mean (SE) from fifteen cross-section images collected from five different plants and significance difference between the genotype was based on student t-test (*$p < 0.05$, **$p < 0.01$, ***$p < 0.001$).

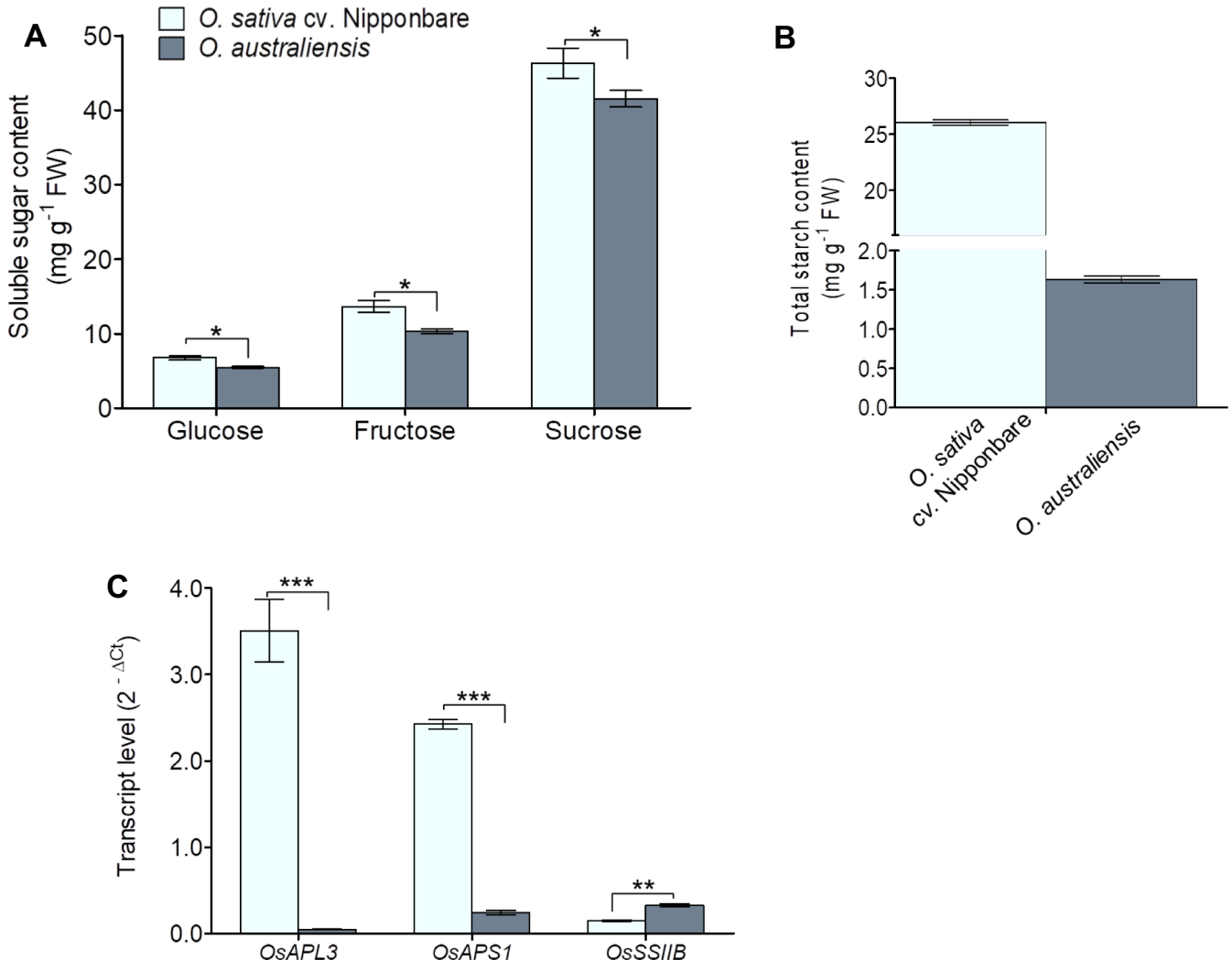

Fig. 5. Quantification of soluble sugars and expression pattern of starch-biosynthesis genes in stems of cultivated rice *O. sativa* cv. Nipponbare and wild rice *O. australiensis* at milk-stage of grain-filling.
(A-B) Glucose, fructose, and sucrose content (A), and total starch content (B) in the stem of the two species (n = 4).
(C) Transcript levels of starch-biosynthesis genes, *OsAPL3* (encoding ADP-glucose pyrophosphorylase large subunit), *OsAPS1* (encoding ADP-glucose pyrophosphorylase small subunit), and *OsSSIIB* (encoding Starch synthase), in the stem of the two species.
Data represents the mean and standard error of mean (SE), and significance difference between the genotype was calculated using student t-test (*$p < 0.05$, **$p < 0.01$, ***$p < 0.001$).

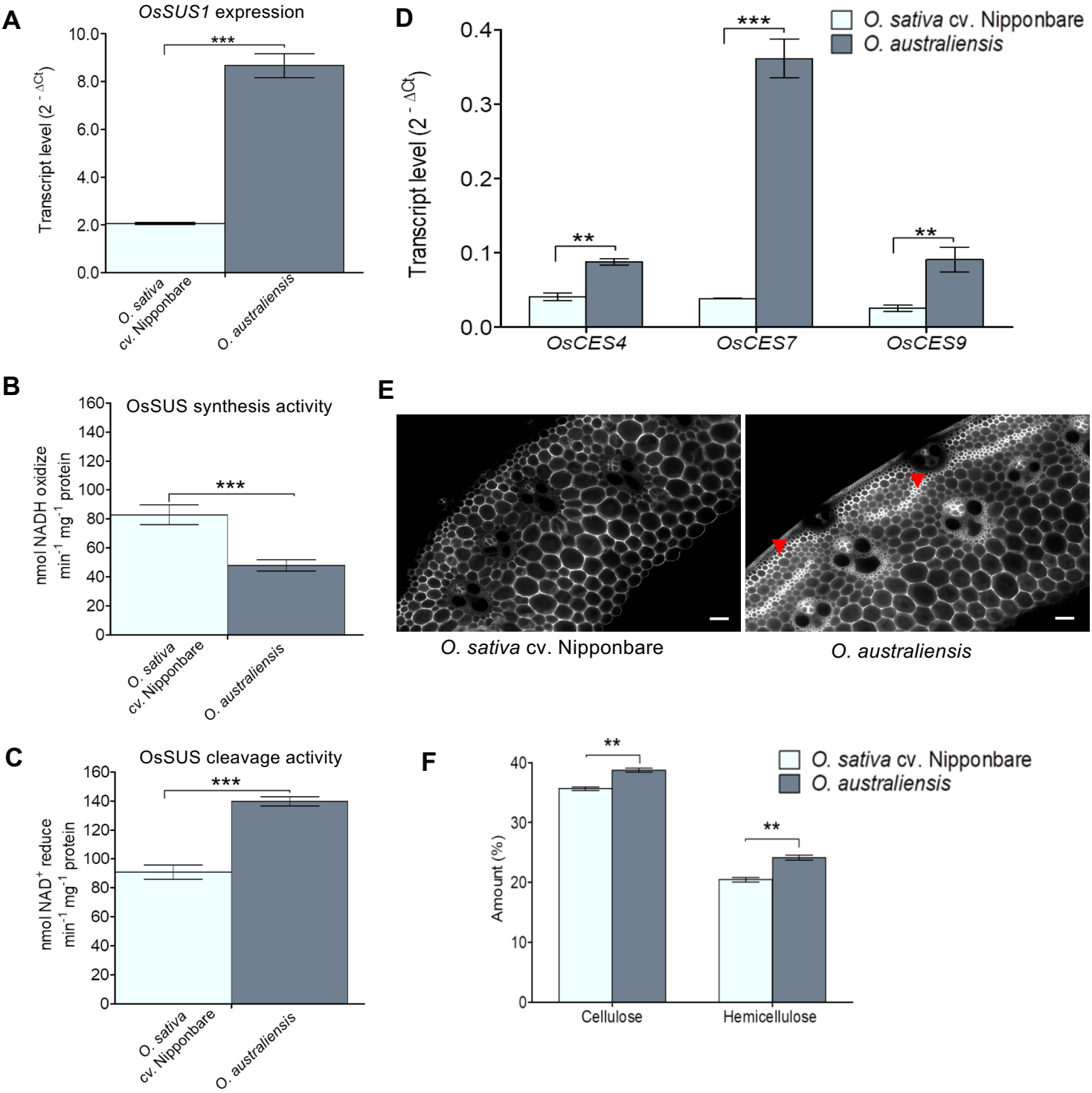

Fig. 6. Expression levels of sucrose metabolism genes, Sucrose Synthase enzyme activity, and structural carbohydrates levels in stem tissue of cultivated rice *O. sativa* cv. Nipponbare and wild rice *O. australiensis* at milk-stage of grain-filling.

(A) Transcript levels of *Sucrose Synthase* 1 (*OsSUS1*).

(B-C) OsSUS enzyme activity in synthesis (B) and cleavage (C) direction.

(D) Transcript levels of *Cellulose Synthase* genes, *OsCES4*, *OsCES7*, and *OsCES9*.

(E) Calcofluor-white staining for cellulose deposition in the transverse stem sections of the two species. Red arrowhead shows higher deposition of cellulose in *O. australiensis* stem. Scale bar represents 500 µm.

(F) Quantification of cellulose and hemicellulose in the stems of the two species.

Data in a- d and f represents the mean and standard error of mean (SE), and significance of difference between the genotype was calculated using student t-test (*$p < 0.05$, **$p < 0.01$, ***$p < 0.001$).

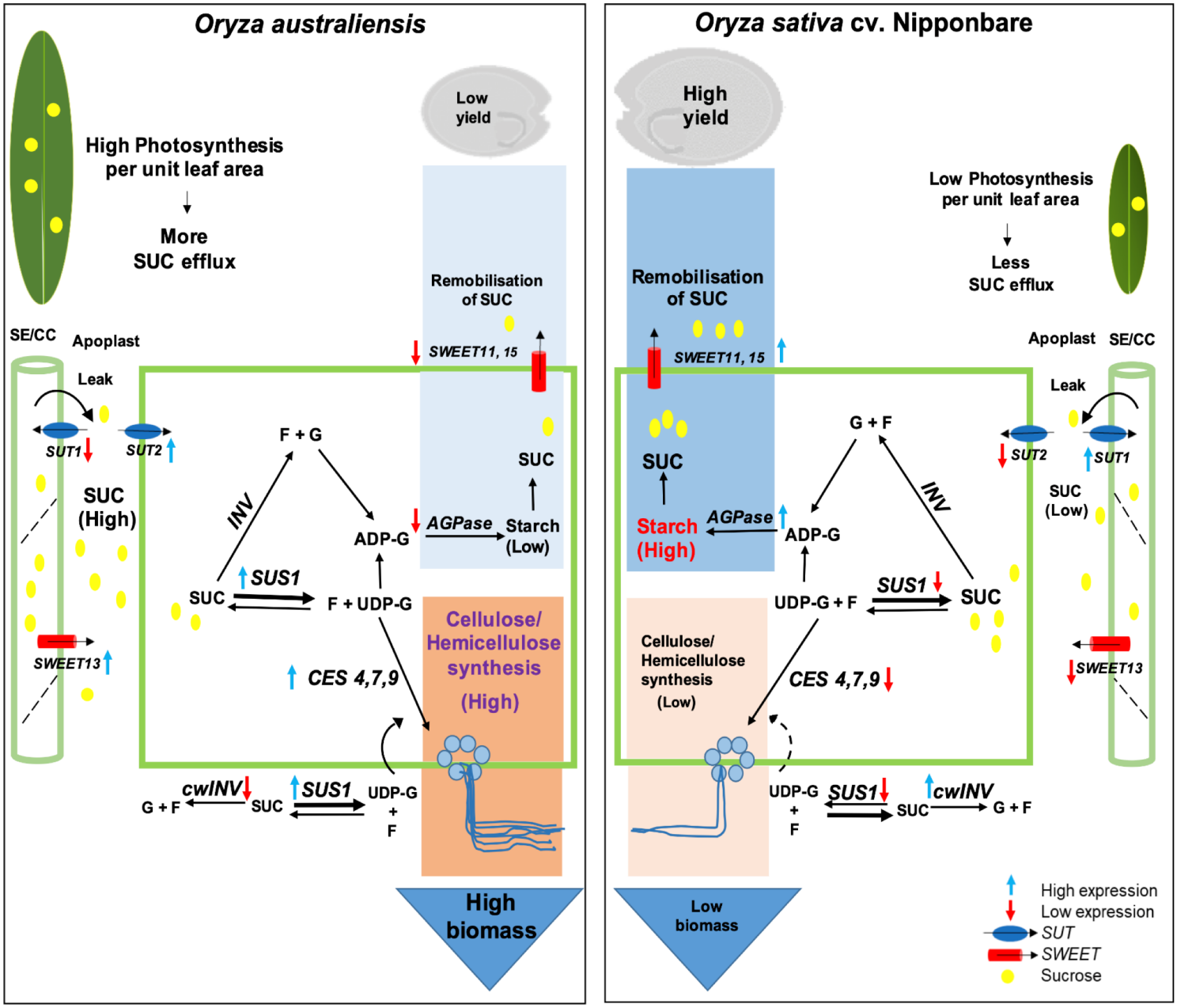

Fig. 7. A model explaining the contribution of sucrose transport, Sucrose Synthase activity, starch biosynthesis, and synthesis of structural carbohydrates towards yield and biomass differences between wild rice *O. australiensis* and cultivated rice *O. sativa* cv. Nipponbare.

High leaf photosynthesis rate coupled with higher expression of selected *OsSWEET* and *OsSUT* genes lead to efficient export of sucrose from leaf in *O. australiensis* compared to *O. sativa* cv. Nipponbare. Sucrose, after getting unloaded to stem due to functions of *OsSWEET13*, *OsSUT1*, and *OsSUT2*, gets converted to UDP-G more efficiently in the wild rice due to higher expression of *OsSUS1* and more cleavage activity of OsSUS compared to the cultivated rice. Higher expression of *OsCES4, OsCES7,*and *OsCES9*, then, leads to more synthesis of cellulose in the stem of the wild rice. In contrast, higher expression of starch-biosynthesis genes, *AGPase* (small and large subunit), leads to higher starch content in the stem of the cultivated rice. Higher synthesis activity of OsSUS along with more expression of *OsSWEET11* and *OsSWEET15* in the cultivated rice facilitate efficient remobilisation of sucrose from stem to panicles at the grain-filling stage. SUC, sucrose (yellow colour circle); F, fructose; G, glucose; UDP-G, UDP-glucose; ADP-G, ADP-glucose; *INV*, Invertase; cwINV, cell wall Invertase; SUS, Sucrose Synthase.